EXPERIMENT MEASUREMENT OF ALFORD'S FORCE

IN AXIAL-FLOW TURBOMACHINERY

John M. Vance
Department of Mechanical Engineering
Texas A&M University
College Station, Texas 77843

Frank J. Laudadio
Motorola Corporation
Fort Lauderdale, Florida 33322

ABSTRACT

In 1965, J. S. Alford published a theory and mathematical model [1] which predicts that circumferential variation of blade-tip clearances in axial-flow turbomachinery will produce cross-coupled (normal to the eccentricity) aerodynamic forces on the rotor. Ever since then, the theory has been used (without experimental verification) by rotor dynamicists as one of the few mathematical models available to calculate the cross-coupled aerodynamic stiffness coefficients required for rotor-dynamic stability analysis.

This paper presents the results of experimental measurements made on a small, high speed, axial flow test apparatus to verify the existence of Alford's force and to investigate the validity of his mathematical prediction model.

INTRODUCTION

There are many mechanisms which cause rotordynamic instabilities in turbines and compressors. An instability in turbomachinery occurs when the shaft precesses about the bearing centerline (whirling) with unacceptable amplitudes, at frequencies nonsynchronous with shaft speed. Instabilities can become a costly problem since they limit the operation of the turbomachinery by reducing the allowable speed. They can be destructive if the instability threshold speed is exceeded.

There are documented cases showing the severity of instabilities in turbomachinery. Doyle [2] presents two cases where an instability has required extensive rotor modification, resulting in lost production and heavy maintenance expenditures. One of the cases mentioned is the 1964 Ekofisk gas reinjection problem which has become a classical example of how costly an instability can become. A centrifugal compressor was designed to reinject the gas by-product from crude oil production. Oil production was stopped for several months due to the instability problem with this compressor.

In mathematical terms an instability occurs when an eigenvalue of the equation that describes the motion of the rotor has a positive real component. In engineering terms, the nonsynchronous amplitude of rotor whirl (any amplitude which has a frequency not equal to running speed) grows with time until the system exceeds its operating limits. In many instances the rotor orbits can be large enough to destroy bearings and seals.

Computer programs are now available [3] which can predict whirling frequencies and threshold speeds, provided that accurate values for the destabilizing coefficients are used as input. The destabilizing coefficients usually take the form of a linearized cross-coupled stiffness term [4], but sometimes are expressed as negative damping [5], depending on the mechanism producing the instability.

One mechanism, which is a type of self-excited instability, is the aerodynamic excitation due to circumferential variation of blade clearance in axial-flow compressors and axial-flow turbines. An objective of the work reported here was to quantify a term in the mathematical equation due to Alford which predicts the magnitude of the aerodynamic cross-coupled stiffness, along with verifying the form of the equation.

Alford actually presented two mechanisms which can cause severe rotor whirl in axial flow compressors and turbines. One is due to the circumferential variation of static pressure action on the cylindrical surface of a rotor, particularly within labyrinth seals. The other is due to circumferential variation of blade-tip clearance (the topic of this paper). Alford presented both seal deflection criteria and bladed-disk torque deflection criteria for use as design guides for a stable rotor system.

Investigations of rotordynamic problems in steam turbines have shown that unbalanced moments on wheels and shafts, caused by steam forces, are a source for nonsynchronous rotor whirl. Steam whirl was first described by Thomas [6] in 1958 and is similar to the phenomenon hypothesized by Alford. Winter [7] performed model tests in 1968. He used ball bearings in his test rig to eliminate the shaft whipping due to hydrodynamic bearings, and applied external damping elements to the bearings since ball bearings have little inherent damping. Winter proved the presence of a load-dependent instability but was not able to quantify his results.

THE TEST APPARATUS

The test apparatus used in the experiment consists of a flexibly mounted bladed rotor driven by a variable speed electric motor, and a movable shroud (see Figure 1). The blade O. D. is 6". The motor is rated 1/7 HP at 10,000 rpm.

An offset of the bladed rotor within the shroud clearance circle is produced by translating the shroud laterally. The shroud is mounted on slides, and is translated laterally by turning a threaded rod.

The lateral stiffness of the rotor bearing support is made low enough so that very low levels of Alford's force (3-10 grams) produce a measurable rotor deflection. The rotor deflection is measured with an eddy-current proximity probe and

calibrated to lateral force in grams/mil. One of the most challenging and time-consuming aspects of the project was the measurement of rotor deflection (DC signal) in the presence of a relative large AC signal produced by rotor runout, synchronous vibration, and ball bearing roughness. This was finally accomplished by passing the probe signal through a very effective low-pass filter.

The speed of the rotor can be varied independently from the torque, over a range of 0 to 7000 rpm, by changing the voltage supplied to the electric motor. The torque is varied by adjusting the air velocity at the rotor inlet with an auxiliary blower. This method allows the rotor speed to be changed while holding the torque constant, or vice versa. Many combinations of speed, torque, and shroud eccentricity can thus be obtained.

Rotor speed is measured by feeding a once-per-revolution keyphaser signal into an electronic counter.

The aerodynamic torque is measured with a strain gage dynamometer. The driving torque of the electric motor is entirely reacted by a steel rod in torsion, with torsional strain gages calibrated to torque.

EXPERIMENTAL PROCEDURE

For each set of data taken, a base measurement was made with the shroud in the center position (i.e. with the lateral eccentricity nominally zero). With the shroud in this position, the rotor was run up to the selected measurement speed and measurements were made of rotor deflection, speed, and torque.

Immediately after completing the base measurements, an eccentricity was imparted to the shroud (adjusting screws translate the shroud laterally) and new values of rotor deflection and torque were measured at the same speed as for the base measurement. Since the direction, as well as the magnitude, of shroud offset was found to have an effect on the measurements, the procedure was repeated for an equal shroud eccentricity in the negative (opposite) direction.

Large quantities of data were taken and averaged, since the repeatability was found to be relatively poor (typically ±20% for two successive measurements of the same variable under the same conditions). The poor repeatability was partially due to apparent aerodynamic instabilities (surging) under some conditions of speed and torque.

RESULTS

The results of the experiments are shown in Figures 2 through 13. The lines connecting the points in the figures were derived using a least squares fit.

Figures 2 and 3 show how the measured Alford force varied with rotor eccentricity. The only difference between the two graphs is in the direction that the eccentricity was imparted. Figures 4 and 5 show the magnitude of the efficiency facor, β, and how it varies with rotor eccentricity. Again, the differnce between the two figures is the direction that the eccentricity was imparted. The efficiency

factor β was calculated using Alford's equation which gives the aerodynamic force as proportional to a radial deflection which is normal to the force. The constant of proportionality is called cross-coupled stiffness. Thus we have

$$F_y = \frac{\tau \beta x}{D_p H} = K_{yx} X \qquad (1)$$

The cross-coupled stiffness is seen to be $K_{yx} = \frac{\tau \beta}{D_p H}$.

Equation (1) implies that β remains constant for varying eccentricity. Figure 5 confirms this. Therefore it was felt that the point on Figure 4 corresponding to 20 mils eccentricity was not representative, and should not be included in the least squares fit.

Figures 6 and 7 show how Alford's force and β vary with torque. Again β was calculated using equation (1). Figure 8 shows how the measured Alford force varied with speed holding the rotor torque constant. Figure 9 was derived from figures 6 and 8. The curve corresponding to 5000 rpm was derived using a least squares fit to the data from all 3 tests in Figure 6. The four remaining curves on Figure 9 were derived from this one curve and Figure 8, using extrapolation techniques. Figures 10, 11, 12 and 13 show how the measured Alford force varied with rotor speed and torque. These figures help support the empirical equation of Alford's force to be presented below. They show how the developed rotor torque varies with the speed.

AN IMPROVED PREDICTION MODEL

One of the remarkable features of Alford's theory is its simplicity. Figures 2, 3, and 6 verify the predicted linearity of Alford's force with rotor eccentricity and stage torque. However, Figure 6 shows that Alford's force does not appear at all until a certain level of stage torque is reached: then it suddenly appears and increases steeply with torque. Alford mentions, in reference [1], that "large power inputs to the compressor rotor appear to increase the hazard of whirl. The vibration problem was encountered only at the full 100 percent power rating of the engine." Figure 6 is compatible with this observation.

Figures 7 and 8 also reveal certain limitations of equation (1), principally that the efficiency factor β actually varies with the aerodynamic load torque and that the developed Alford's force is speed-dependent as well as torque-dependent. Also, extrapolation of the curves for Alford's force versus torque (e.g. Figure 6) shows that the y-intercept is not zero as equation (1) predicts.

To obtain an improved prediction model, the speed must be included as a pertinent variable. Dimensional analysis shows that if the speed is pertinent, then the inlet velocity is also pertinent. In dimensionless groups, the prediction equation takes the form

$$\frac{F_y D_p}{\tau} = f \left(\frac{x}{H}, \frac{D_p}{H}, \frac{V}{N D_p} \right) \qquad (2)$$

263

where N = speed, rpm
       V = inlet velocity, fps
       and the other variables are as previously defined.

In the experiments reported here, measurements of the inlet velocity V were not made. Therefore the improved prediction model at this stage must be purely empirical, to fit the available test data.

Equation (1) is modified to include a y-intercept, which gives

$$F_y = \frac{\tau \beta x}{D_p H} + C \tag{3}$$

where the constant C is evaluated as C = -17.37 from Figure 9.

In addition, Figure 9 shows that the slope of the curve is affected by the rotor speed. A relationship can be calculated between the rotor speed and the slope $x/(D_p H)$, as follows:

$$\frac{\beta x}{D_p H} = -10.54 \times 10^{-3} \text{ (N)} + 89.33 \tag{4}$$

Substituting equation (4) into equation (3) gives

$$F_y = (-10.54 \times 10^{-3} \text{ (N)} + 89.33) \tau - 17.37 \tag{5}$$

In a more general form; factoring out $x/(D_p H)$ where x = 40 mils, D_p = 4.875 in., and H = 0.875 in. gives

$$F_y = \left\{ (-1.12(N) + 9526.42) \tau - 1852.35 \right\} \frac{x}{D_p H} \tag{6}$$

where
F_y = Alford force, grams
τ = developed rotor torque, in-lb
N = rotor speed, rpm
x = eccentricity, in
D_p = blade diameter, in
H = bucket height, in

If the units of Alford force are taken to be pounds (lb), the equation becomes

$$F_y = \left\{ (-2.47 \times 10^{-3}(\text{rpm}^{-1}) \times (N) + 21.0) \tau - 4.08(\text{in-lb}) \right\} \frac{x}{D_p H} \tag{7}$$

Equation (6) reasonably approximates all of the curves presented in this paper that show Alford's force as a function of developed rotor torque, rotor speed, and eccentricity. It is a purely empirical equation which fits the measured data for the described test rig.

264

CONCLUSIONS AND SUGGESTIONS FOR FUTURE RESEARCH

Due to the size of the test rig and the lack of measurement capability for aerodynamic velocities and pressures, the conclusions which can be made from this research are quite limited in scope. They are as follows:

1. The aerodynamic force postulated by Alford for axial flow turbomachinery does exist, and can be measured experimentally.

2. Alford's force is speed-dependent as well as torque-dependent, and is probably also a function of the gas velocity entering the stage.

3. Although the relationship of Alford's force to the stage torque is fairly linear at a given speed, the y-intercept is not zero. That is, no aerodynamic force is generated until a certain level of stage torque is reached.

The authors believe that these conclusions are significant, since rotordynamics engineers have used Alford's theory for years with no experimental verification.

However, it is easy to see why rotordynamic stability thresholds cannot be reliably predicted at present by computer analyses which use Alford's equation as a model for the destabilizing coefficients. In order to do this, it will be necessary to develop more accurate prediction models for the aerodynamic force, which will require experimental measurements on full scale turbomachinery components, such as an axial flow stage from the compressor in a turbojet aircraft engine, or an industrial process compressor.

REFERENCES

1. Alford, J. S., "Protecting Turbomachinery from Self-Excited Rotor Whirl," Journal of Engineering for Power, Vol. 87, Series A, No. 4, October 1965, pp. 333-334.

2. Doyle, H. E., "Field Experiences with Rotordynamic Instability in High-Performance Turbomachinery," Proceedings of a Workshop held at Texas A&M University, May 1980, NASA Conference Publication 2133.

3. Murphy, B. T., "Computer Programs for Critical Speeds and Stability Analysis," Rotordynamics of Turbomachinery Short Course, Texas A&M University, May 18-20, 1981.

4. Vance, J. M. and Laudadio, F. J., "Rotordynamic Instabilities in Centrifugal Compressors - Are all the Excitations Understood?", ASME Journal of Engineering for Power, April 1981, pp. 288-293.

5. Vance, J. M., "Instabilities in Turbomachinery", Proceedings of the 5th Annual Vibration Institute Seminar on Machinery Vibration Analysis, April 9, 1981, New Orleans, La.

6. Thomas, H. J., "Unstable Oscillations of Turbine Rotors Due to Steam Leakage in the Clearances of the Sealing Glands and the Buckets," Bulletin Scientifique, A. J. M. 71, 1958, pp. 1039-1063.

7. Winter, C. J., "Instabile Bewegungen von Turbinenlaeufern infolge lastabhaengiger Erregerkraefte," Energie and Technik, January 1969, pp. 7-13.
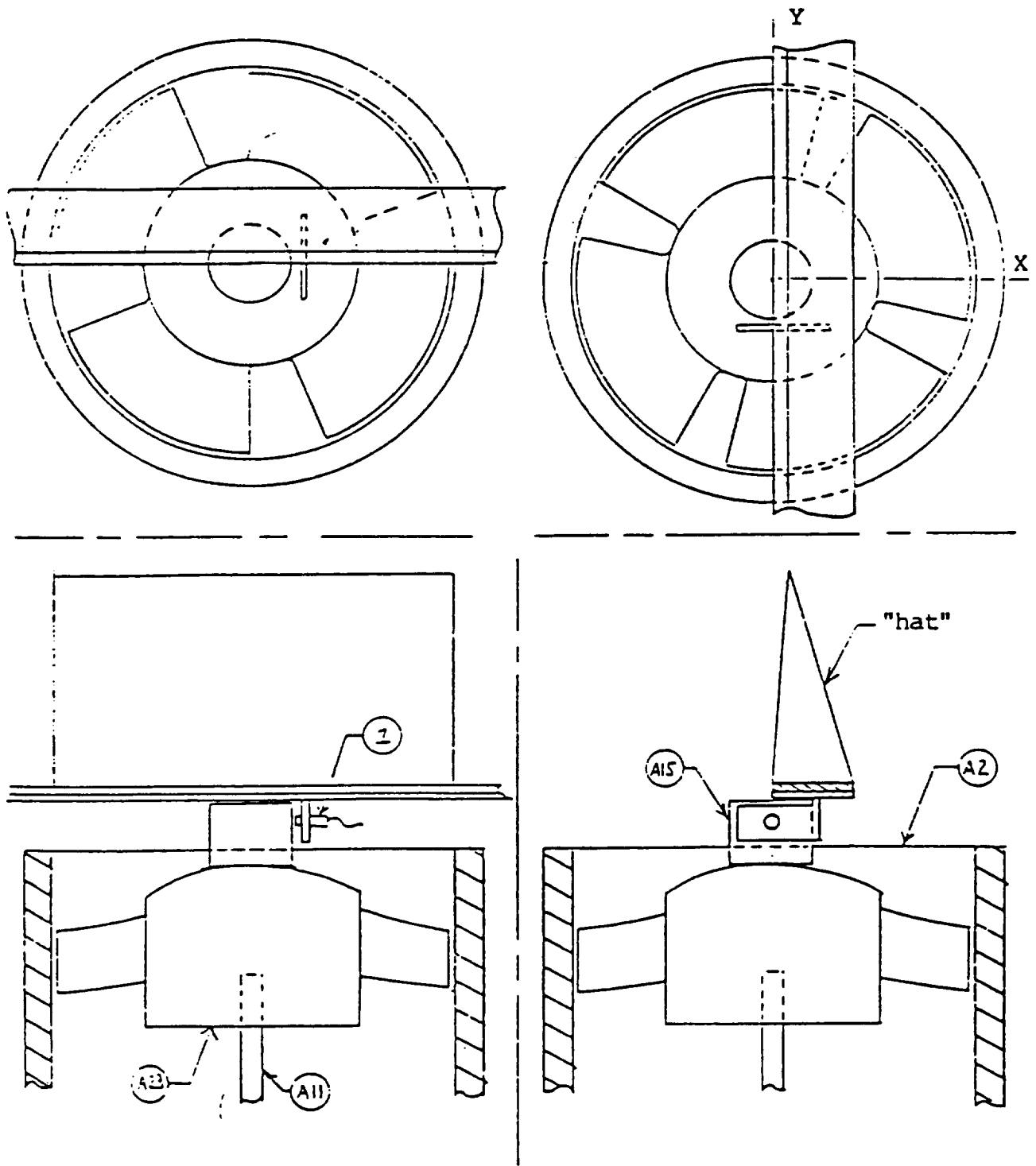
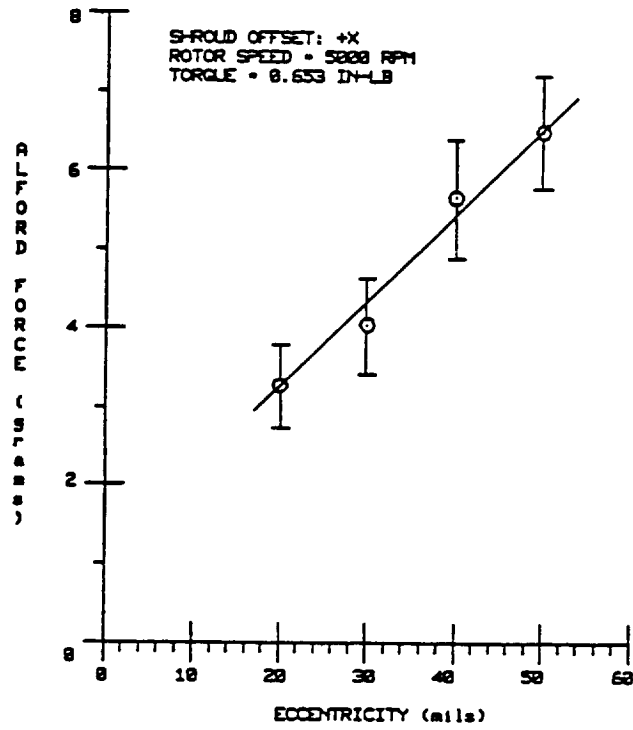Figure 1. - Drawing of top of test rig showing inlet configuration and coordinate system.

Figure 2. - Alford force as function of rotor eccentricity, showing ±2 standard deviations (shroud offset: +X).
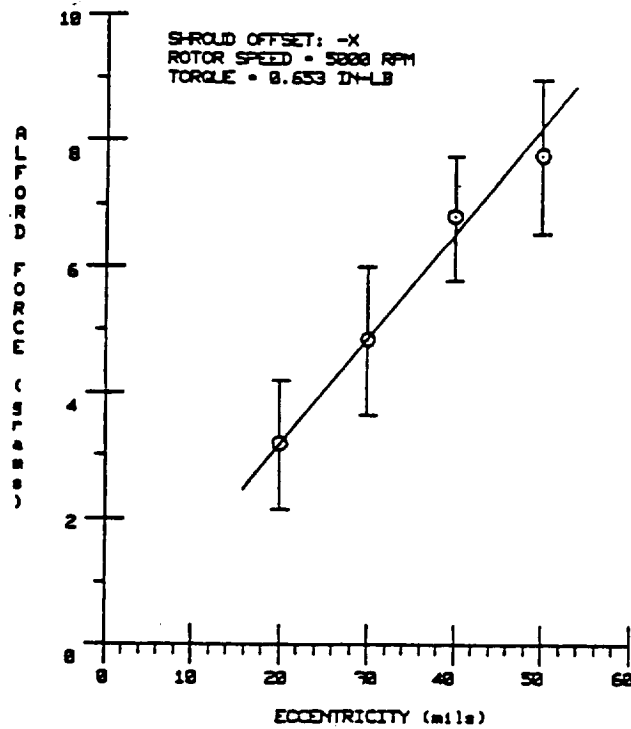
Figure 3. - Alford force as function of rotor eccentricity, showing ±2 standard deviations (shroud offset: -X).

268
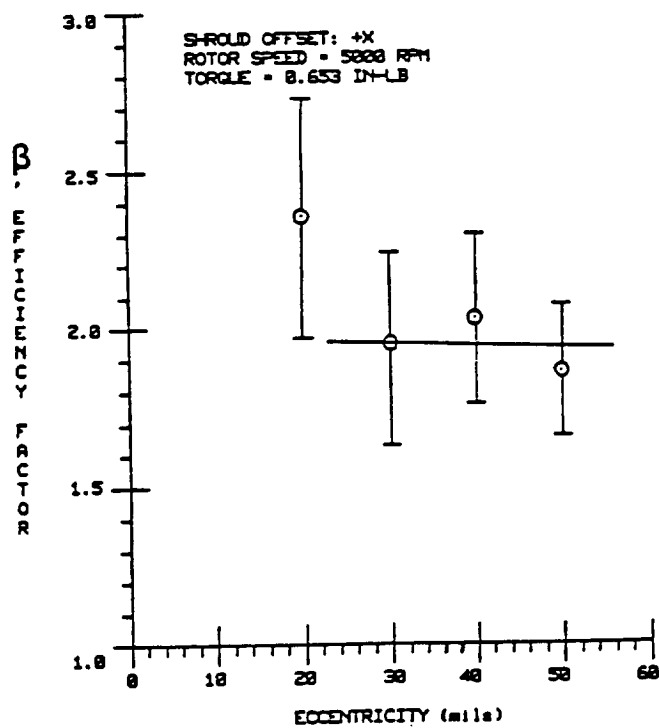
Figure 4. - Efficiency factor, β, as function of rotor eccentricity, showing
±2 standard deviations (shroud offset: +X).
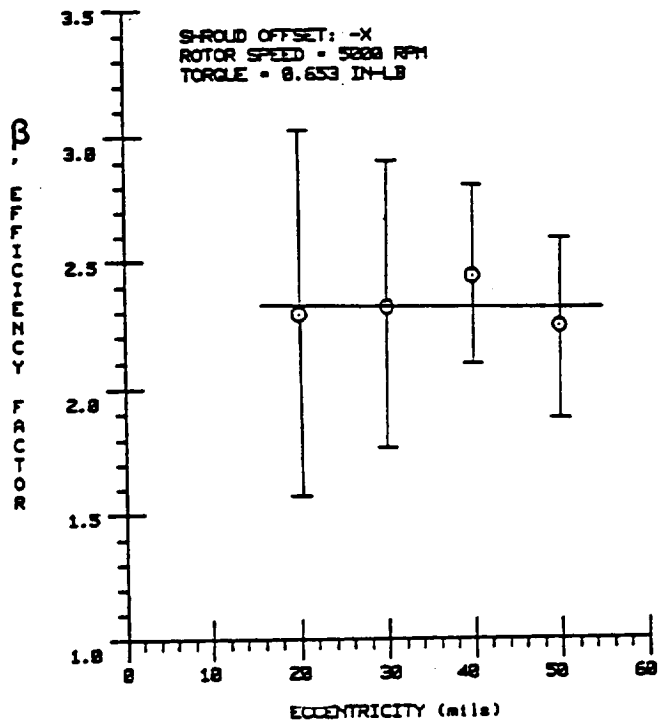
Figure 5. - Efficiency factor, β, as function of rotor eccentricity, showing
±2 standard deviations (shroud offset: -X).
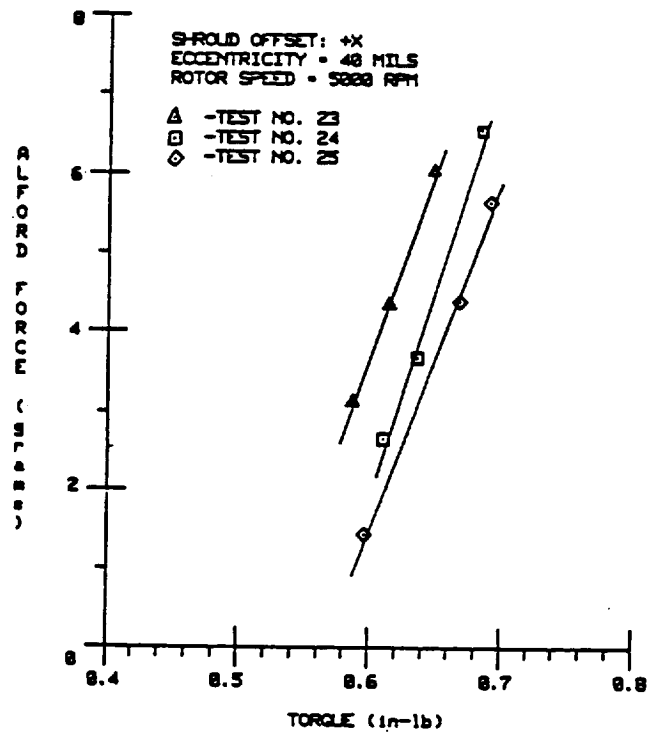
Figure 6. - Alford force as function of developed rotor torque (for three different tests).
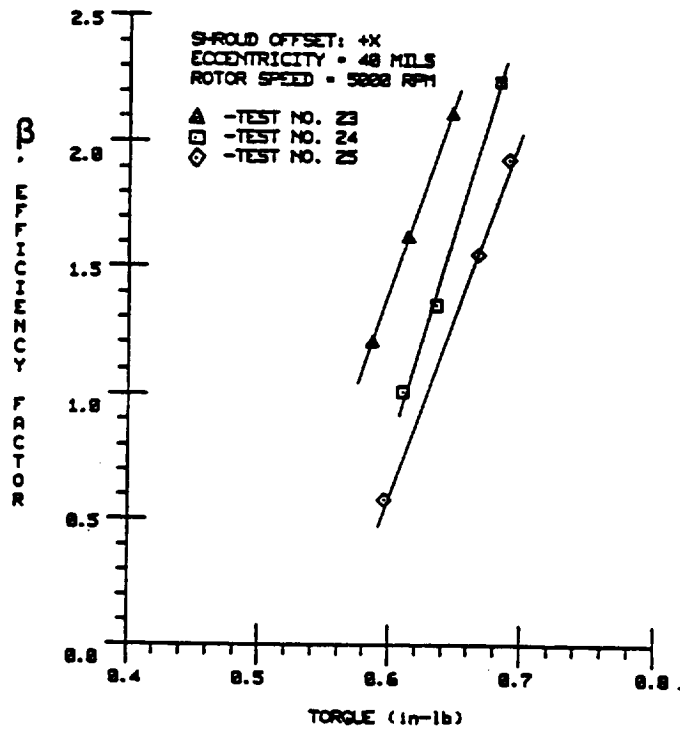
Figure 7. - Efficiency factor, β, as function of developed rotor torque (for three different tests).
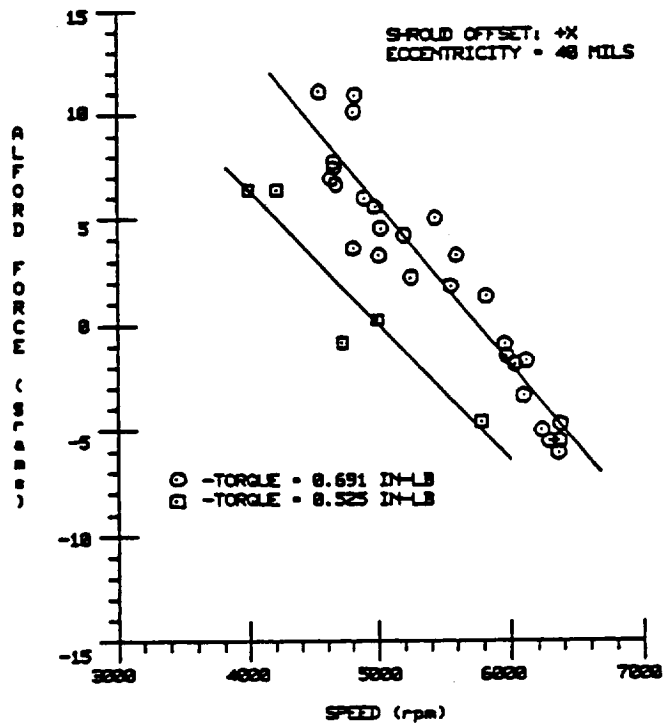
Figure 8. - Alford force as function of rotor speed (for two different values of torque).
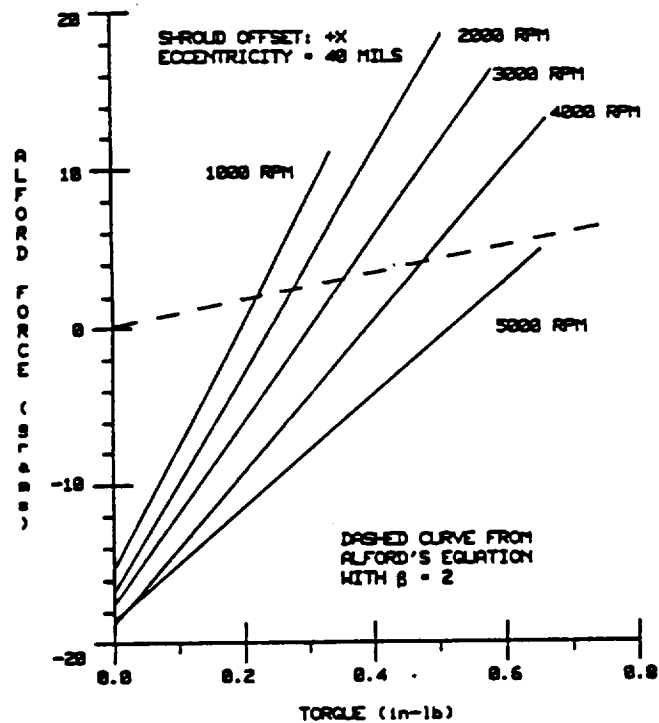
Figure 9. - Alford force as function of developed rotor torque (for different values of speed).
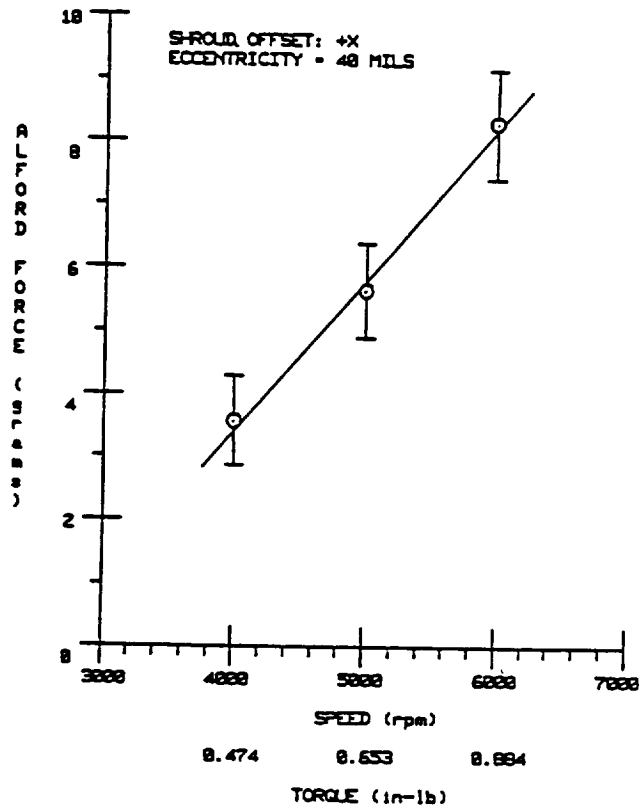
271

Figure 10. - Alford force as function of developed rotor torque and rotor speed, showing ±2 standard deviations (shroud offset: +X).
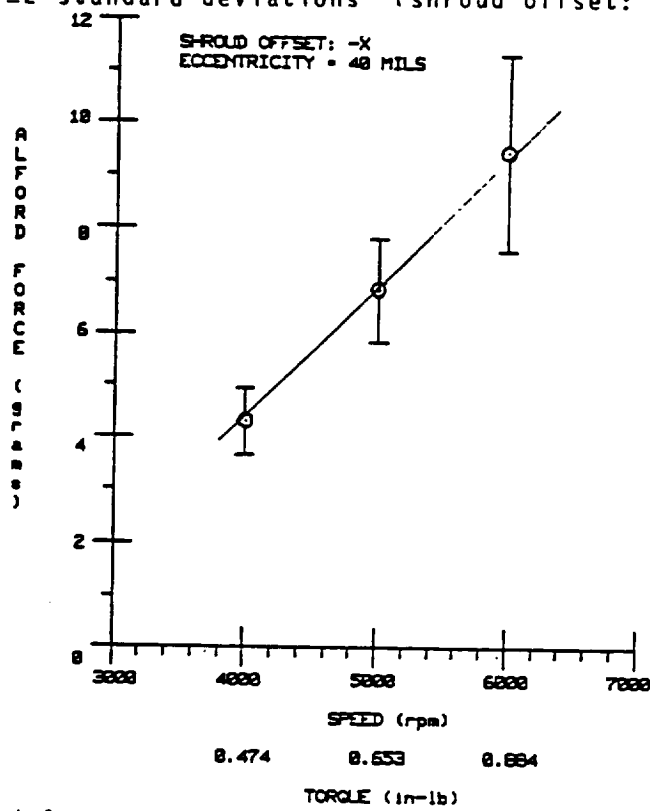

Figure 11. - Alford force as function of developed rotor torque and rotor speed, showing ±2 standard deviations (shroud offset: -X).
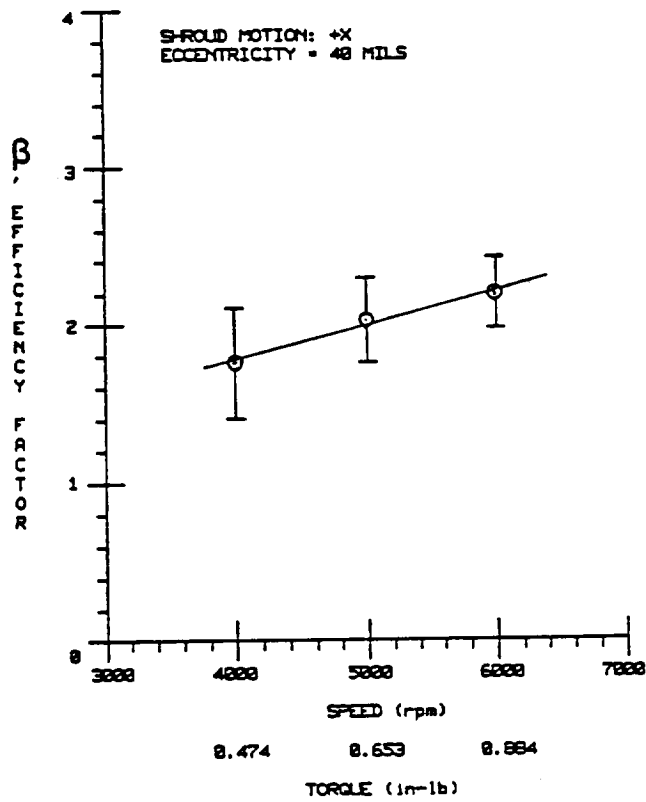
272

Figure 12. - Efficiency factor, β, as function of developed rotor torque and rotor speed, showing ±2 standard deviations (shroud offset: +X).
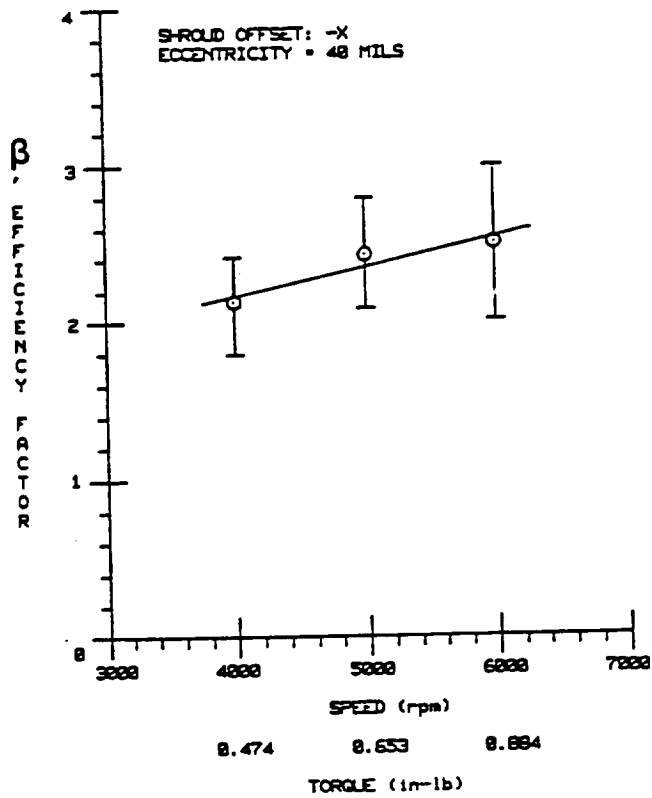

Figure 13. - Efficiency factor, β, as function of developed rotor torque and rotor speed, showing ±2 standard deviations (shroud offset: -X).